PROCEEDINGS OF SCIENCE

arXiv:1512.00282v1 [hep-lat] 1 Dec 2015

The Rho Resonance from $N_f = 2+1+1$ Twisted Mass Lattice QCD

C. Helmes, C. Jost, B. Knippschild, L. Liu, C. Urbach, M. Werner*
HISKP (Theory), University of Bonn, Nussallee 14-16, Bonn, Germany
E-mail: werner@hiskp.uni-bonn.de

Z. Wang

School of Physics, Peking University, Beijing, China

for the European Twisted Mass Collaboration

We present first results on the ρ resonance parameters obtained with $N_f = 2+1+1$ Wilson twisted mass fermions at maximal twist. Using ensembles of the ETM collaboration, we provide results for two values of the lattice spacing and a range of pion mass values.

The 33rd International Symposium on Lattice Field Theory
14 -18 July 2015
*Kobe International Conference Center, Kobe, Japan**

*Speaker.

© Copyright owned by the author(s) under the terms of the Creative Commons Attribution-NonCommercial-NoDerivatives 4.0 International License (CC BY-NC-ND 4.0).

name	L/a	T/a	N_{conf}	a[fm]	M_π[MeV]
A30.32	32	64	147	0.086	147
A40.32	32	64	250	0.086	250
A60.24	24	48	245	0.086	246
A80.24	24	48	251	0.086	254
B55.32	32	64	146	0.082	146

Table 1: All Ensembles are generated by the European Twisted Mass Collaboration with $N_f = 2+1+1$ Wilson twisted mass fermions [1, 2]

1. Introduction

The ρ resonance is located in the isospin-1 channel of $\pi\pi$ scattering. The ρ decays strongly almost exclusively into $\pi\pi$. It is besides the f_0 or σ resonance the lowest resonance in QCD. Therefore, it is highly desirable to gain theoretical insight using a non-perturbative method like lattice QCD.

Resonance properties are not directly accessible in lattice QCD due to the Euclidean structure of space-time [3]. Martin Lüscher invented an approach utilising finite size effects in energy levels of multi-particle states, which can be directly related to the infinite volume scattering phase shift.

In this proceeding we present preliminary results of the first calculation of the ρ resonance properties using lattice QCD with $N_f = 2+1+1$ dynamical quark flavours. The computation is based on gauge configurations generated by the European Twisted Mass Collaboration (ETMC) [1, 2] and uses the Wilson twisted mass discretisation of QCD [4], which has the property of automatic $\mathcal{O}(a)$ improvement [5] at so-called maximal twist. Details of the gauge configurations used including the spatial and temporal lattice extends L/a and T/a, respectively, and the number of configurations N_{conf} can be found in table 1. For more details we refer to the corresponding references from which we also took over the notation. For other results on the ρ meson from this conference see Refs. [6, 7].

2. Lüscher Method

The relation between energy levels in a finite volume and the infinite volume phase shift was first described by Lüscher in Refs. [8, 9, 10, 11]. It was later on extended and generalised for moving frames [12, 13]. In this paper we follow the notations of Ref. [14]. In a general moving frame with momentum $\vec{P} = 2\pi\vec{n}/L$, one first computes the energy E of the $\pi\pi$ system with $I = 1$ for the interacting case using suitable operators as described in the next section. Next, the center-of-mass frame energy

$$E_{\text{CM}}^2 = E^2 - \vec{P}^2$$

and the corresponding Lorentz factor

$$\gamma = \frac{E}{E_{\text{CM}}}$$

are computed. From the center-of-mass energy the lattice-momentum transfer fraction, q, can be derived via

$$\tilde{q}^2 = \frac{E_{\mathrm{CM}}^2}{4} - M_\pi^2, \qquad q^2 = \left(\frac{\tilde{q}L}{2\pi}\right)^2,$$

where M_π is the pion rest mass. With the definition of γ and q it is possible to connect the finite-volume energies with phase shift values via

$$w_{lm} = \frac{1}{\pi^{3/2}\sqrt{2l+1}} \gamma^{-1} q^{-l-1} \mathscr{Z}_{lm}^{\vec{n}}(q^2). \tag{2.1}$$

where $\mathscr{Z}_{lm}^{\vec{n}}(q^2)$ is the generalised Lüscher $\mathscr{Z}$-function. For example, the phase shift in the center of mass frame ($\vec{n} = 0, \gamma = 1$), δ_1, is obtained via [11]

$$\cot \delta_1 \;=\; w_{00}. \tag{2.2}$$

Similar relations hold also for moving frames, see e.g. Ref. [14].

In principle mixing with higher partial waves needs to be taken into account but it has been shown in Ref. [15] that the mixing is negligible in practice. We will assume this holds for our data at the moment. Nevertheless, we will investigate the validity of this assumption in the future.

The experimental data for the scattering phase shift $\delta_1(E_{\mathrm{CM}})$ can be described using the effective range formula [16]

$$\tan \delta_1(E_{\mathrm{CM}}) \;=\; \frac{g_{\rho\pi\pi}^2}{6\pi} \frac{\tilde{q}^3}{E_{\mathrm{CM}}(M_\rho^2 - E_{\mathrm{CM}}^2)}, \tag{2.3}$$

with two parameters, the effective coupling $g_{\rho\pi\pi}$ and the ρ meson mass M_ρ, respectively. Following Ref. [13], we are going to use this formula to describe our lattice data for the scattering phase shift $\delta_1(E_{\mathrm{CM}})$. M_ρ and $g_{\rho\pi\pi}$ are related to the ρ meson decay width Γ_ρ by

$$\Gamma_\rho \;=\; \frac{g_{\rho\pi\pi}^2 \left(M_\rho^2/4 - M_\pi^2\right)^{\frac{3}{2}}}{6\pi M_\rho^2}, \tag{2.4}$$

with M_π the pion mass.

3. Operators and Data Analysis

We determine the interacting energy levels E by computing the following 2×2 correlation matrix

$$\mathscr{C}(\vec{P},t) = \langle \vec{O} \otimes \vec{O}^\dagger \rangle, \qquad \vec{O} = (\pi\pi(\vec{P},t), \rho^0(\vec{P},t))^t. \tag{3.1}$$

The interpolating operators $\pi\pi(\vec{P},t)$ and $\rho^0(\vec{P},t)$ are the two particle and single particle operators, respectively, which couple to the isospin-1 channel depending on the total center of mass momentum $\vec{P}$. For details on the construction of these operators see e.g. Refs. [13, 15]. For this proceeding we concentrate on the A_1 irreducible representation of the octahedral group [14]. We include all frames with $\vec{n}^2 = 0,1,2,3$, including all possible permutations contribution to the same $\vec{n}^2$.

As a smearing scheme we use the stochastic Laplacian Heaviside method as described in Refs. [17, 18]. The details and our parameter choices can be found in Ref. [19].

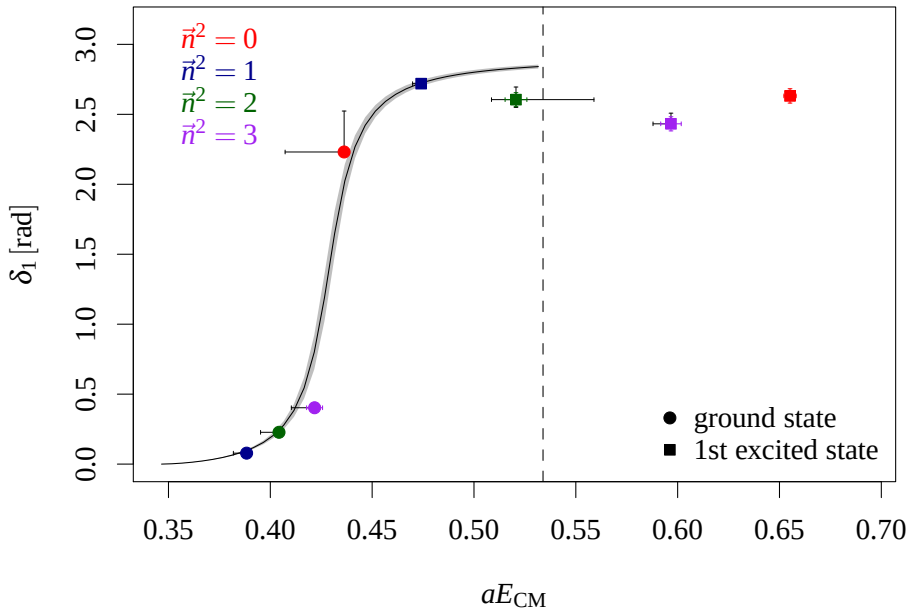


Figure 1: $I = 1$ $\pi\pi$ scattering phase shift for the A60 ensemble. The solid line is a fit of the effective range formula Eq. 2.3 to our data with statistical errors indicated by the band. The vertical line indicates the $2M_K$ threshold.

Note that in Wilson twisted mass lattice QCD isospin is broken explicitly at $\mathcal{O}(a^2)$ which leads to fermionic disconnected contributions to the ρ^0. These contributions are pure lattice artefacts and will, therefore, be neglected in our analysis, see also Ref. [13].

Next we solve the generalised eigenvalue problem

$$\mathscr{C}(t)\ \eta^{(n)}(t,t_0) = \lambda^{(n)}(t,t_0)\ \mathscr{C}(t_0)\ \eta^{(n)}(t,t_0)$$

for eigenvectors $\eta^{(n)}(t,t_0)$ and eigenvalues $\lambda^{(n)}(t,t_0)$, $n = 0,1$ [20, 21]. The energy levels are determined from the exponential fall-off of $\lambda(t,t_0)$ at large t-values. Each 2×2 correlation matrix allows us to access two energy levels. We take the so-called thermal pollutions [22] into account by weighting and shifting of $\mathscr{C}$ [15].

The analysis follows the one we already described in Ref. [19]. We use a bootstrap procedure with 5000 bootstrap samples to compute statistical errors and to estimate the variance-covariance matrix used in the χ^2-fits. For a given eigenvalue we fit an exponential function with two free parameters to the data for a large set of fit ranges $[t_1,t_2]$ with degrees of freedom larger than 5 for the lowest energy level and larger than 4 for the first excited state. The p-value of each fit indicates whether or not this model is justified. The energy level is, therefore, determined as the weighted

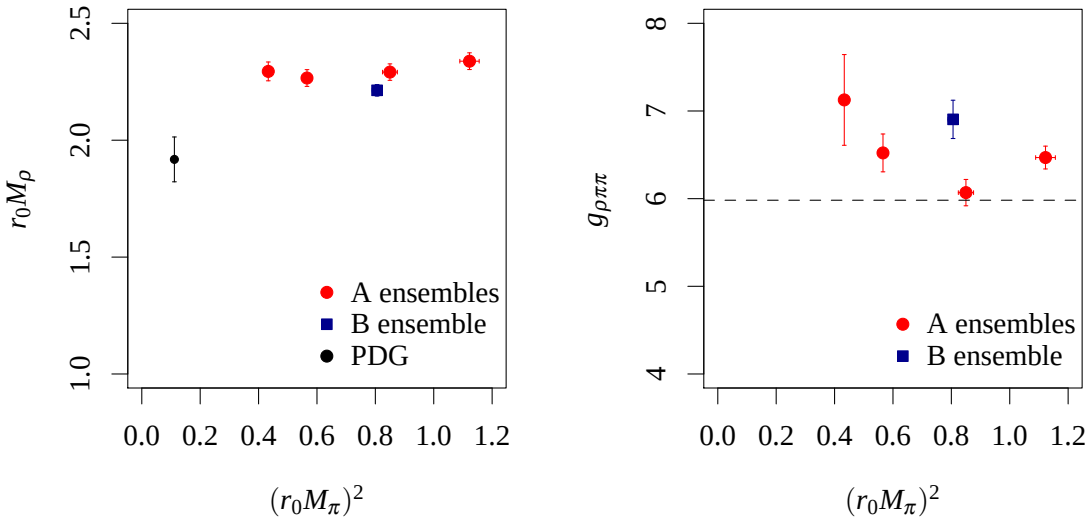


Figure 2: Left: ρ resonance mass $r_0 M_\rho$ as a function of the squared pion mass $(r_0 M_\pi)^2$ for all ensembles investigated in this work. The black point is the corresponding PDG value [23]. Right: $g_{\rho\pi\pi}$ versus the squared pion mass $(r_0 M_\pi)^2$. The dashed horizontal line corresponds to the PDG value.

median over all used fit ranges with weight [19]

$$w_{\mathrm{E}} = \{(1-2|p_{\mathrm{E}}-0.5|)\cdot 1/\Delta_{\mathrm{E}}\}^2\,,$$

where p_{E} is the p-value of the corresponding exponential fit and Δ_{E} the statistical error of the energy level determined from the bootstrap procedure. Similarly, we determine the pion mass M_π and derived quantities like δ_1, see Ref. [19]. In the computation of δ_1 we exclude energy levels where $E_{\mathrm{CM}} < 2M_\pi$, which might appear due to statistical fluctuations. A systematic uncertainty on E and δ_1 stemming from the fit ranges is obtained from the 68% confidence interval of the corresponding weighted distributions.

4. Results

In figure 1 we show the P-wave scattering phase shift as a function of aE_{CM} for the A60.24 ensemble (cf. Table 1) below inelastic threshold. We show statistical errors as the inner error bars and the systematic error as the outer error bars in the figure. As visible, the systematic uncertainties are sizable in some cases which is a hint that we do not yet control excited or thermal states satisfactorily with the weighting and shifting procedure. In the future we will increase the operator basis to get a better handle on these effects.

We observe that – as expected for a resonance – the phase-shift starts around 0, rises sharply through $\pi/2$ around $aE_{\mathrm{CM}} = 0.43$ and levels out again somewhat below 3. The fit of Eq. 2.3 to

the data is shown in figure 1 as the solid line with error band. Statistical errors on E_{CM} and δ_1 are included correlated in the fit, while systematic uncertainties are not yet included. All points in the range from $2M_\pi$ to $2M_K$ are included in the fit. The fit describes the data well, though the χ^2 value is not particularly good. This comes mainly from the decrease in δ_1 at E_{CM} close to $2M_K$. We observe a similar behaviour on all our ensembles. The large χ^2-value might also be due to not completely removed excited or thermal states, which we are currently investigating. Note, however, that the χ^2 value reduces already significantly once systematic uncertainties are included in the fit.

We have carried out this analysis for all ensembles listed in table 1. We remark that the ensembles B55.32 and A30.32 currently have significantly lower statistics than the other three ensembles. The resulting values of M_ρ are shown in units of the Sommer parameter r_0 in the left plot of figure 2 as a function of $(r_0 M_\pi)^2$. The values and errors of r_0/a are taken from Ref. [24]. The errors of r_0 are propagated via parametric bootstrap to $r_0 M_\rho$. Additionally, we show the PDG value of $M_\rho = 775.5\,\mathrm{MeV}$ [23] using $r_0 = 0.49(2)$ fm. The error on this point is solely coming from the uncertainty in the physical value of r_0. In the right plot of figure 2 we show $g_{\rho\pi\pi}$ again as a function of $(r_0 M_\pi)^2$. The uncertainties of $g_{\rho\pi\pi}$ are significantly larger than for M_ρ due to the structure of the ERF Eq. 2.3. The experimental value of $g_{\rho\pi\pi}$ included in the figure was obtained by inserting $M_\rho = 775.5\,\mathrm{MeV}$, $\Gamma_\rho = 149.1\,\mathrm{MeV}$ and $M_\pi = 139.57\,\mathrm{MeV}$ into Eq. 2.4. Within the currently still sizable uncertainties for the effective coupling we can confirm the mild dependence on M_π^2 observed in previous lattice investigations. Note that we did not yet estimate a systematic uncertainty for M_ρ and $g_{\rho\pi\pi}$.

5. Summary and Outlook

We have presented first results of the ρ meson resonance properties obtained with $N_f = 2+1+1$ Wilson twisted mass fermions. The computations have been performed for two values of the lattice spacing and a range of pion mass values.

For a number of ETMC ensembles we have determined the scattering phase shift δ_1 as a function of the center of mass energy. Using the effective range formula, we obtain the ρ resonance mass M_ρ and the effective coupling $g_{\rho\pi\pi}$. This study will be extended by enlarging the operator basis and by including more irreducible representations which will help to investigate systematic errors stemming from excited or thermal states further. To analyse lattice artifacts and perform a chiral extrapolation we will increase the number of lattice spacing values and pion masses.

We thank the members of ETMC for the most enjoyable collaboration. The computer time for this project was made available to us by the John von Neumann-Institute for Computing (NIC) on the JUDGE and Juqueen systems in Jülich. We thank U.-G. Meißner for granting us access on JUDGE. This project was funded by the DFG as a project in the Sino-German CRC110. Z. Wang was supported in part by the National Science Foundation of China (NSFC) under the project o.11335001. The open source software packages tmLQCD [25], Lemon [26] and R [27] have been used.

References

[1] R. Baron *et al.,* JHEP **06**, 111 (2010), arXiv:1004.5284.

[2] ETMC, R. Baron *et al.*, PoS **LATTICE2010**, 123 (2010), arXiv:1101.0518.

[3] L. Maiani and M. Testa, Phys.Lett. **B245**, 585 (1990).

[4] ALPHA, R. Frezzotti, P. A. Grassi, S. Sint, and P. Weisz, JHEP **08**, 058 (2001), hep-lat/0101001.

[5] R. Frezzotti and G. C. Rossi, JHEP **08**, 007 (2004), hep-lat/0306014.

[6] J. Bulava *et al.*, Pion-pion scattering and the timelike pion form factor from $N_\mathrm{f} = 2+1$ lattice QCD simulations using the stochastic LapH method, in *Proceedings, 33rd International Symposium on Lattice Field Theory (Lattice 2015)*, 2015, arXiv:1511.02351.

[7] D. Guo and A. Alexandru, Resonance Parameters for the rho-meson from Lattice QCD, in *Proceedings, 33rd International Symposium on Lattice Field Theory (Lattice 2015)*, 2015, arXiv:1511.06334.

[8] M. Lüscher, Commun.Math.Phys. **104**, 177 (1986).

[9] M. Lüscher, Commun.Math.Phys. **105**, 153 (1986).

[10] M. Lüscher, Nucl.Phys. **B354**, 531 (1991).

[11] M. Lüscher, Nucl. Phys. **B364**, 237 (1991).

[12] K. Rummukainen and S. A. Gottlieb, Nucl.Phys. **B450**, 397 (1995), arXiv:hep-lat/9503028.

[13] X. Feng, K. Jansen, and D. B. Renner, Phys. Rev. **D83**, 094505 (2011), arXiv:1011.5288.

[14] M. Gockeler *et al.*, Phys. Rev. **D86**, 094513 (2012), arXiv:1206.4141.

[15] Hadron Spectrum, J. J. Dudek, R. G. Edwards, and C. E. Thomas, Phys. Rev. **D87**, 034505 (2013), arXiv:1212.0830, [Erratum: Phys. Rev.D90,no.9,099902(2014)].

[16] L. S. Brown and R. L. Goble, Phys. Rev. Lett. **20**, 346 (1968).

[17] Hadron Spectrum, M. Peardon *et al.*, Phys. Rev. **D80**, 054506 (2009), arXiv:0905.2160.

[18] C. Morningstar *et al.*, Phys.Rev. **D83**, 114505 (2011), arXiv:1104.3870.

[19] ETMC, C. Helmes *et al.*, JHEP **09**, 109 (2015), arXiv:1506.00408.

[20] C. Michael and I. Teasdale, Nucl.Phys. **B215**, 433 (1983).

[21] M. Lüscher and U. Wolff, Nucl.Phys. **B339**, 222 (1990).

[22] X. Feng, K. Jansen, and D. B. Renner, Phys.Lett. **B684**, 268 (2010), arXiv:0909.3255.

[23] Particle Data Group, K. A. Olive *et al.*, Chin. Phys. **C38**, 090001 (2014).

[24] ETMC, N. Carrasco *et al.*, Nucl.Phys. **B887**, 19 (2014), arXiv:1403.4504.

[25] K. Jansen and C. Urbach, Comput.Phys.Commun. **180**, 2717 (2009), arXiv:0905.3331.

[26] ETMC, A. Deuzeman, S. Reker, and C. Urbach, Comput. Phys. Commun. **183**, 1321 (2012), arXiv:1106.4177.

[27] R Development Core Team, *R: A language and environment for statistical computing*, R Foundation for Statistical Computing, Vienna, Austria, 2005, ISBN 3-900051-07-0.